arXiv:cond-mat/0507182v1 [cond-mat.stat-mech] 7 Jul 2005

Conformation-networks of two-dimensional lattice homopolymers

Yu-Pin Luo[a], Hung-Yeh Lin[a], Ming-Chang Huang[a], and Tsong-Ming Liaw[b]
[a]Department of Physics, Chung-Yuan Christian University,Chungli 320,Taiwan
[b]Computing Center, Academia Sinica, Nankang 115, Taiwan

December 28, 2021

Abstract

The effect of different Monte Carlo move sets on the the folding kinetics of lattice polymer chains is studied from the geometry of the conformation-network. The networks have the characteristics of small- world. The Monte Carlo move, rigid rotation, has drastic effect on the geometric properties of the network. The move not only change the connections but also reduce greatly the shortest path length between conformations. The networks are as robust as random network.

Protein folding is a complex process for which, a sequence of amino acids folds into a unique and stable structure in a relatively short time[1]. The lattice models have been used widely as coarse-grained models for the theoretical study of folding process[2, 3, 4, 5, 6, 7]. In the lattice models, protein is viewed as a chain of m monomers, and the conformations are given by all possible self-avoiding walks of the chain on two-dimensional ($2D$) or three-dimensional ($3D$) regular lattices. The energy of a conformation generally depends on the number of intrachain contacts, and how to assign the contact energy is model dependent. The kinetics of the folding process then is studied by Monte Carlo simulations for which, a move set is designed for the change of conformations. In principle, different move sets, satisfying the requirement of ergodicity, should reach the same equilibrium canonical distribution after sufficiently long time simulations. However, different move sets may yield different perspectives of folding kinetics. The question of how different move sets affect folding kinetics was discussed before by Chan and Dill[5, 6]. Based on two different sets, they used transfer matrix with Metropolis criterion to study the folding kinetics of two-dimensional homo- and hetero-polymers. The results indicate that the kinetic sequence of folding events and the shape of the energy landscape depend strongly on the move set. Hoang and Cieplak also obtained the same conclusions after comparing the dynamics of three different move sets[8]. Therefore, it is important to understand the nature of a move set adopted in the lattice dynamics.

The purpose of this Letter is to explore the characteristics of different move sets from the geometric properties of the corresponding conformation-networks[9, 10]. We study the conformation spaces of the homopolymers with $m \leq 16$ on the $2D$ square lattice for different move sets. Though the chain lengths considered in this work are relatively short, we can construct the networks by exact enumeration. For the conformation-networks obtained by different move sets, firstly, what are the characteristic features of the networks? It was shown by Scala et. al.[10] that the geometric properties of the conformation-network obtained from the mapping of a particular conformation space are similar to those of small-world networks. A small-world network is characterized by two properties: the local connection is as cliquy as regular lattices, and the characteristic path length increases logarithmically with the number of nodes[11, 12]. Do the conformation-networks obtained from different move sets all have the characteristics of small-world networks? For this, we analyze the characteristic path lengths and clustering coefficients of the networks. Then, what are the differences in the geometric properties of the networks? This leads us to the analyses of the distribution functions of the edge number per node and the shortest path lengths between two nodes. Finally, we also discuss the stability of the networks.

For the dynamical simulations of lattice polymers, the typical Monte Carlo moves include (i) end flips, (ii) corner shift, (iii)crankshaft move, and (iv) rigid rotation, as shown in Fig. 1. Based on these moves, we consider three different move sets, **SA**, **SB**, and **SC**, which are defined as the followings. The moves, (i), (ii), and (iii), which change only one or two monomers in a move, are relatively local in comparison with the move (iv). Because of the locality, these moves have been adopted very often in the literatures[7, 13, 14]. We refer these moves as **SA**. Note that **SA** may not satisfy the requirement of ergodicity: In the case of $2D$ square lattice, all exactly enumerated conformations are reachable for $m < 16$, there is one unreachable for $m = 16$, and the unreachable number may become large for $m > 16$[5, 6, 8]. The move (iv) contains the change of more monomers, and it makes some simple diffusive motions for groups of monomers to be possible[15]. Since the move (i) can be viewed as a short-scale rigid rotations, we then combine the move (iv) with the move (i) to form the set of rotational moves, **SB**. Note that the move (ii) or (iii) from a conformation can be achieved by two or more sequential moves of **SB**, and all unreachable conformations for **SA** can be obtained by the moves of **SB**. Thus, **SA** may be viewed as a subset of **SB**. Finally, we refer the move set containing all the moves as **SC**.

Based on the move sets **SA**, **SB**, and **SC**, we construct the respective conformation-networks as the followings: First, we enumerate all possible self-avoiding conformations $N(m)$ as the nodes of the network for the chain of m monomers. Note that the degeneracy caused by the rotation and the mirror symmetry has been excluded in $N(m)$. Then, edges exist between two nodes for which a move of the given move set can change one to the other. The move sets, **SA**, **SB**, and **SC**, yield different distributions of edges among the nodes and hence different networks. The networks can be viewed as the folding networks in high temperature limit, all edges have the same weight. We refer the

resultant networks as **GA**, **GB**, and **GC** for the move sets, **SA**, **SB**, and **SC**, respectively. The numbers of nodes $N(m)$ and the numbers of edges $E(m)$ of different networks for different number of monomers m are listed in Table 1.

Firstly, we analyze the edge distributions of the networks. The number of edges associated with a node is the number of allowed transitions from one conformation to the others. The spread in the number of edges is characterized by a distribution function $P(k)$ which gives the probability for a node to have k edges. Then, the average edge-number per node is given by

$$\langle k \rangle = \sum_k kP(k). \tag{1}$$

The results of $\langle k \rangle$ are listed in Table 1, and they all scale as $\langle k \rangle = a + b \log(N(m))$, shown in the insets of Fig. 2, with (a, b) given as $(3.79, 0.92)$ for **GA**, $(3.07, 2.99)$ for **GB**, and $(2.77, 4.01)$ for **GC**. Thus, the average edge-number per node generated by the move set **SB** (**SC**) is about three (four) times the average number generated by **SA**. This gives more throughway accessibility to the native conformation and reduces the chance to be trapped in local minimum in the folding process for the move sets **SB** and **SC**[5, 6].

Our results of $P(k)$ versus $\Delta k = k - \langle k \rangle$ for **GA**, **GB**, and **GC** with $m = 10$, 12, 14, and 16 are shown in Figs. 2(a), 2(b), and 2(c), respectively. Amaral et. al. studied the subnetwork of **GA** for which, the end-to-end distance is a parameter with a specified value for a network and the edges between nodes are generated by the moves, corner shift and crankshaft move[9, 10]. Their results showed that the form of $P(k)$ is Gaussian. Then, we find the best fittings of the Gaussian function,

$$P(k) = \frac{1}{\sqrt{2\pi}\sigma} \exp\left[-\frac{(k - \langle k \rangle)^2}{2\sigma^2}\right], \tag{2}$$

for **GA**, **GB**, and **GC**, as the solid lines in Fig. 2. Our results indicate the followings: (i) For **GA**, the distribution agrees with the Gaussian form for which, the average of the variances of different m is $\sigma_{\mathbf{GA}} = (0.5748)\sqrt{N_m}$. (ii) Comparing with the case of **GA**, there are significant deviations from the Gaussian form for the cases of **GB** and **GC** as shown in Figs. 2(b) and 2(c), but the distributions are obviously not scale-free[16, 17, 18].

The degree of local connections of the networks can be measured by the clustering coefficients. We define the clustering coefficient of the node i as

$$C_i = \frac{2E_{k_i}}{k_i(k_i + 1)}, \tag{3}$$

where k_i is the edge-number and E_{k_i} is the existent edge-number among the neighboring k_i nodes of the node i. Then, the degree of local connections of the network can be characterized by the average of the clustering coefficients of the nodes, denoted by C_{av}. The values of C_{av} for **GA**, **GB**, and **GC** with different m values are listed in Table 1. The results show $C_{av}^{GA} > C_{av}^{GB} > C_{av}^{GC}$, and this

implies that the Monte Carlo simulation with the move set **SA** has more chances to be trapped in some clinquy conformations comparing with those of **SB** and **SC**. For the network with the node-number N and the average edge-number $\langle k \rangle$, the corresponding random network has the average clustering coefficient $C_{av}^{ran} \approx \langle k \rangle / N$. The results of the ratios of C_{av} of **GA**, **GB**, and **GC** to C_{av}^{ran} are shown in Fig. 3, and they indicate that the average clustering coefficients of the conformation-networks are much larger than that of random network.

Then, we analyze the path lengths between two nodes of the network. The minimum number of Monte Carlo moves required for one conformation to reach the other can be viewed as the distance between two conformations[5, 6]. Thus, the shortest path length l between two nodes can be defined as the minimum number of edges required to connect the two nodes. Our results indicate that the distribution functions of the shortest path lengths, $P(l)$, of different networks all agree with the Gaussian form of Eq. (2). In Fig. 4 we plot the scaled results of the distribution function, $\widetilde{P}(l) = \sqrt{2\pi}\sigma P(l)$, versus $\widetilde{\Delta l} = (l - \langle l \rangle)/\sqrt{2}\sigma$ for **GA**, **GB**, and **GC**, with $m = 10$, 12, 14, and 16. Here, we take the variances σ as $\sigma_{\mathbf{GA}} = 0.0489\,(m)^{1.7}$, $\sigma_{\mathbf{GB}} = 0.3057\,(m)^{0.6}$, and $\sigma_{\mathbf{GC}} = 0.5057\,(m)^{0.6}$, which are determined by first finding the least square fit to Eq. (2) to obtain $\sigma(m)$ for a given m, and then taking the average over $\sigma(m)$ of different m to obtain σ for a given network. The variance of $P(l)$ for **GB** is much smaller than that for **GA**, and this implies that the shortest distance between any two nodes does not vary much for the networks **GB** and **GC**.

The characteristic path length of the network, $\langle l \rangle$, is defined as the average of the shortest path lengths for all node-pairs,

$$\langle l \rangle = \sum_{l} l P(l). \tag{4}$$

The values of $\langle l \rangle$ for **GA**, **GB**, and **GC** with different m values are listed in Table 1. The results indicate that the characteristic path length of **GB** is about half of the length of **GA**. For the small-world networks, there exists a cross-over size N^*,which is about the same order as the inverse of the rewiring probability p,such that the characteristic path lengths $\langle l \rangle$ obey the finite-size scaling low[19, 20, 21],

$$\langle l \rangle = (N^*)^{1/d} f\left(\frac{N}{N^*}\right), \tag{5}$$

where d is the dimensionality of the underlie regular lattice, and $f(x)$ is a scaling function with the limits, $f(x) \sim x^{1/d}$ for $x \ll 1$ and $f(x) \sim \ln x$ for $x \gg 1$. By taking the hypothesis that the conformation network may be a small-world network, we use the scaling form of Eq. (5) to fit the data, and the results are shown in Fig. 5. The fittings indicate that (i) the values of $\langle l \rangle$ increase logarithmically with the node-number N for large N; (ii) we obtain $1/d$ from the fittings of small N as 0.3427, 0.2377, and 0.2155 for the networks **GA**, **GB**, and **GC** respectively, and then our estimations of d are $d_{GA} \sim 3$, $d_{GB} \sim 4$, and $d_{GC} \sim 4.5$; and (iii) the cross-over region $N^*(m)$ is around $m = 9 \sim 11$ $\left(p \sim 10^{-3} - 10^{-4}\right)$ for **GA** and 8 $\left(p \sim 10^{-3}\right)$ for **GB** and **GC**.

Note that we do not take the data from $m \leq 4$ for which the node-number N is less than 5, and thence the data points available for the region of small N are few. Based on the above results, we may conclude that the dimensionality of the conformation-space is $d \geq 3$, and the cross-over region become narrower when the dimensionality gets larger.

Finally, we analyze the ability of attack and error tolerance of the network by studying the fragmentation caused by node-removal[22]. The nodes with higher degrees of connections are removed preferentially for the analysis of attack tolerance; and the nodes are removed randomly for the error tolerance. By removing a fraction f of the nodes, we measure the fraction of nodes contained in the largest cluster, S, and the average node number, $\langle s \rangle$, contained in the fragmentary clusters excluding the largest one. If only the removed nodes were missing from without further breaking the largest cluster, the S value decreases from 1 down to 0 along the diagonal line as f increases from 0 up to 1; and the $\langle s \rangle$ value remains to be one for $0 < f \leq 1$ if the removed nodes were isolated from each other. For most networks, we may expect that while as the S values start to decrease more rapidly than the diagonal line at some fraction f_m, and drop to zero at the critical fraction f_c; the $\langle s \rangle$ value start to increase more rapidly from $\langle s \rangle = 1$ at f_m, and reach the maximum at f_c. The results of S and $\langle s \rangle$ as function of f are shown in Fig. 6 for the networks **GA**, **GB**, and **GC** with $m = 16$. Our results show that the f_c value is very closed to 1, and the stability of the networks is very analogous to random networks.

In summary, we divide the frequently used Monte Carlo moves into three different move sets, and construct the corresponding conformation-networks. The networks all have the characteristics of small- world: (i) the local neighborhood is more cliquy than that of random networks, and (ii) the characteristic path length increases logarithmically with the number of nodes. The dimensionalities of the conformation-spaces are $d \geq 3$. Our analyses also indicate that the networks are as robust as random graphs. Among different Monte Carlo moves, the rigid rotation has drastic effect on the geometric properties of the network: (i) it renders the connection distribution to be non-Gaussian, and (ii) it reduces greatly the characteristic path length. Thus, the Monte Carlo move, rigid rotation, may change the folding kinetics significantly from that of the local moves, corner shift and crankshaft move.

Acknowledgments

This work was partially supported by the National Science Council of Republic of China (Taiwan) under the Grant No. NSC93-2212-M033-005. We thank National Center for High-performance Computing and the Computing Centre of Academia Sinica for providing the computation facilities.

References

[1] T.E. Creighton (ed.), Protein Folding (Freeman,New York, 1992).

[2] J. Skolnick and A. Kolinski, Annu. Rev. Phys. Chem. **40**, 207(1989).

[3] E. Shakhnovich, G. Farztdinov, A.M. Gutin, and M. Karplus, Phys. Rev. Lett. **67**, 1665(1991).

[4] R. Miller, C.A. Danko, J. Fasolka, A.C. Balazs, H.S. Chan, and K.A. Dill, J. Chem. Phys. **96**, 768(1992).

[5] H.S. Chan and K.A. Dill, J. Chem. Phys. **99**, 2116(1993).

[6] H.S. Chan and K.A. Dill, J. Chem. Phys. **100**, 9238(1994)

[7] A. Sali, E. Shakhnovich, and M. Karplus, J. Mol. Biol. **235**, 1614(1994).

[8] T.X. Hoang and M. Cieplak, J. Chem. Phys. **109**, 9192(1998).

[9] L.A.N. Amaral, A. Scala, M. Barthélémy, and H.E. Stanley, Proc. Natl. Acad. Sci. USA **97**, 11149(2000).

[10] A. Scala, L.A.N. Amaral, and M. Barthélémy, Europhys. Lett. **55**,594(2001).

[11] D.J. Watts and D.H. Strogatz, Nature (London) **393**, 440(1998).

[12] D.J. Watts, Small Words: The Dynamics of Networks Between Order and Randomness, (Princeton Univ. Press, Princeton, NJ 1999).

[13] N.D. Socci and J.N. Onuchic, J. Chem. Phys. **101**, 1519(1994); **103**, 4732(1995).

[14] R. Melin, H. Li, N.S. Wingreen, and C. Tang, J. Chem. Phys. **110**, 1252(1999).

[15] J. Skolnick and A. Kolinski, J. Mol. Bio. **235**, 1614(1994).

[16] A.-L. Barabási and R. Albert, Science **286**, 509(1999).

[17] R. Albert, H. Jeong, and A.-L. Barabási, Nature (London) **401**, 130(1999).

[18] H. Jeong, B. Tombor, R. Albert, Z.N. Oltavi, and A.-L. Barabási, Nature **407**, 651(2000).

[19] M. Barthélémy and L.A.N. Amaral, Phys. Rev. Lett. **82**, 3180(1999); **82**, 5180(E)(1999).

[20] A. Barrat, e-print cond-mat/9903323(1999).

[21] M.E.J. Newman and D.J. Watts, Phys. Lett. A**263**, 341(1999).

[22] R. Albert, H. Jeong, and A.-L. Barabási, Nature (London) **406**, 378(2000); **409**, 542(E)(2001).

Figure 1: Examples of typical Monte Carlo moves: (a) end flips, (b) corner shift, (c)crankshaft move, and (d) rigid rotation. The current conformation is shown in thick lines, and possible new conformations are shown in broken lines.

Table 1: Various geometric quantities of the conformation-networks **GA**, **GB**, and **GC** with different number of monomers m: the numbers of nodes N, the numbers of edges E, the average edge number per node $\langle k\rangle$, and the characteristic path length $\langle l\rangle$.

m	10	12	14	16
N	2034	15037	110188	802075
E^{GA}	6966	57451	464687	3702485
E^{GB}	13194	117839	1005304	8314161
E^{GC}	16397	147673	1268544	10554679
$\langle k\rangle^{GA}$	6.8496	7.6413	8.4344	9.2323
$\langle k\rangle^{GB}$	12.9735	15.6732	18.2471	20.7316
$\langle k\rangle^{GC}$	16.1229	19.6413	23.0251	26.3184
$\langle l\rangle^{GA}$	7.6369	11.0731	15.0046	19.4403
$\langle l\rangle^{GB}$	4.5953	5.8286	7.0726	8.3236
$\langle l\rangle^{GC}$	3.9555	4.9611	5.9723	6.9869

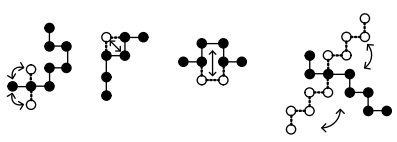
Figure 2: The probability distribution of edges, $P(k)$, versus $\Delta k = k - \langle k \rangle$ for the networks (a)**GA**, (b)**GB**, and (c)**GC**. Here, $\langle k \rangle$ is the average edge number per node, and the solid lines are the best fittings of the Gaussian function given in the text. For each network, $\langle k \rangle$ versus $\log(N(m))$ for the node number $N(m)$ with the monomer number m ranged from 8 to 16 is shown in the inset, and the straight solid line corresponds to the relation $\langle k \rangle = a + b \log(N(m))$ with the values of a and b given in the text.

Figure 3: The ratios of the average clustering coefficients, C_{av}, of the networks **GA**, **GB**, and **GC** to the average clustering coefficients of random lattices C_{av}^{ran} versus $\log(N)$ with the node number $N(m)$ and the monomer number m ranged from 8 to 16.

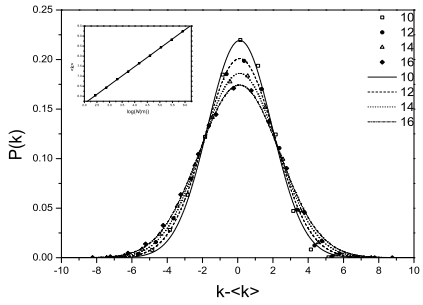
Figure 4: The scaled result of the distribution function of the shortest path lengths $P(l)$, $\widetilde{P}(l) = \sqrt{2\pi}\sigma P(l)$, versus $\widetilde{\Delta l} = (l - \langle l \rangle)/\sqrt{2}\sigma$ for (a) **GA**, (b) **GB**, and (c)**GC**, with $m = 10$, 12, 14, and 16. The averages of the shortest path lengths for all node-pairs $\langle l \rangle$ are given in Table 1, and the variances σ are $\sigma_{\mathbf{GA}} = 0.0489\,(m)^{1.7}$, $\sigma_{\mathbf{GB}} = 0.3057\,(m)^{0.6}$, and $\sigma_{\mathbf{GC}} = 0.5057\,(m)^{0.6}$. The solid lines are the results of the Gaussian function given in the text.

Figure 5: The characteristic path length $\langle l \rangle$ versus the logarithm of the node-number N, $\log(N)$, for the networks (a) **GA**, (b) **GB**, and (c) **GC** with the monomer number m ranged from 5 to 16. The insets are the plots of $\log(\langle l \rangle)$ versus $\log(N)$ for the same data. The solid lines are the results of the limiting scaling forms given in the text.

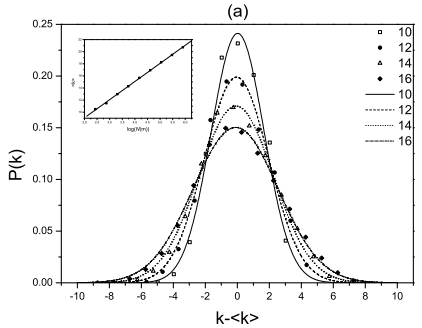
Figure 6: The fraction of nodes contained in the largest cluster, S, and the average node number, $\langle s \rangle$, contained in the fragmentary clusters excluding the largest one versus the fraction f of the nodes removed for (a) attack and (b) error tolerance of the networks **GA**, **GB**, and **GC** with $m = 16$.



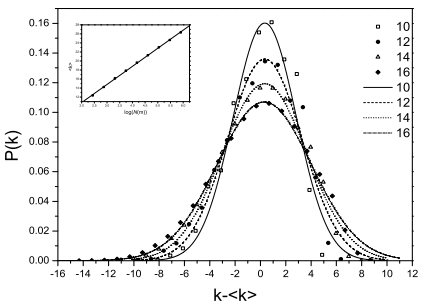
(a) (b) (c) (d)


P(k)
k-<k>
10
12
14
16
10
12
14
16

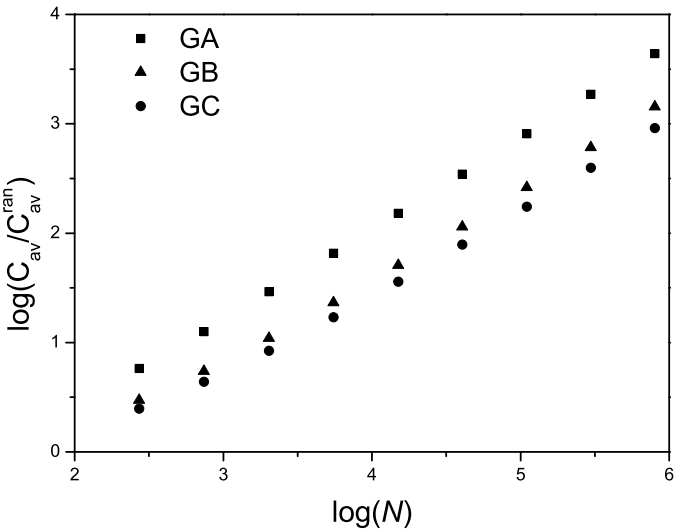
(a)

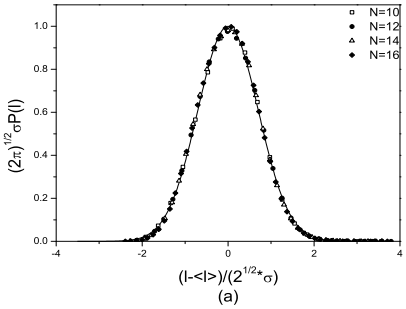

P(k)
k-<k>
10
12
14
16
10
12
14
16

(b)

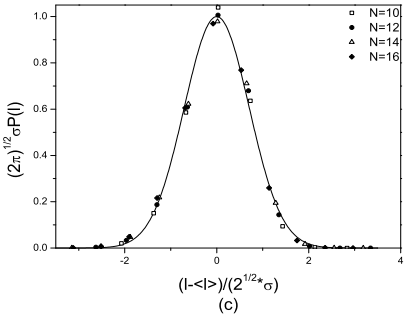

P(k)
k-<k>
10
12
14
16
10
12
14
16

(c)

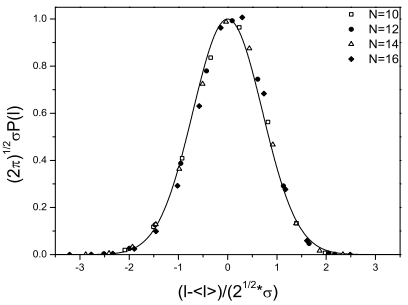

GA
GB
GC
log(C_{av}/C^{ran}_{av})
log(N)
0
1
2
3
4
2
3
4
5
6


N=10
N=12
N=14
N=16
$(2\pi)^{1/2}\sigma P(l)$
$(l-<l>)/(2^{1/2}*\sigma)$

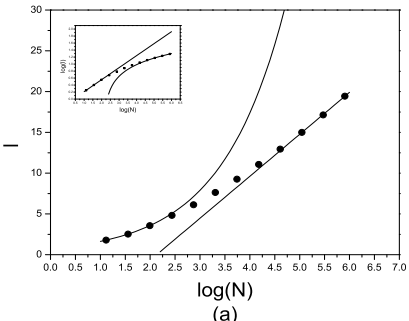
(a)

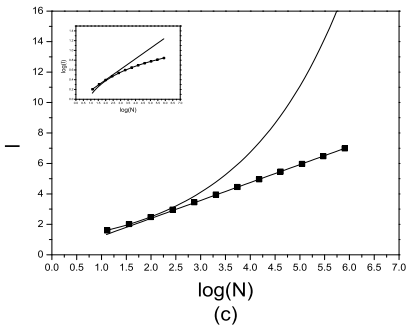

N=10
N=12
N=14
N=16
$(2\pi)^{1/2}\sigma P(l)$
$(l-<l>)/(2^{1/2}*\sigma)$

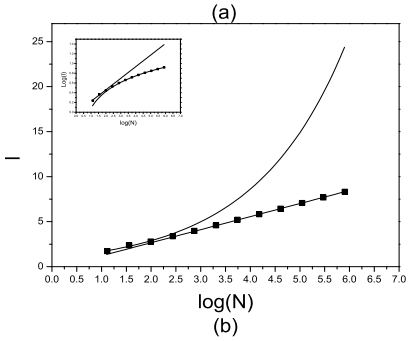
(c)

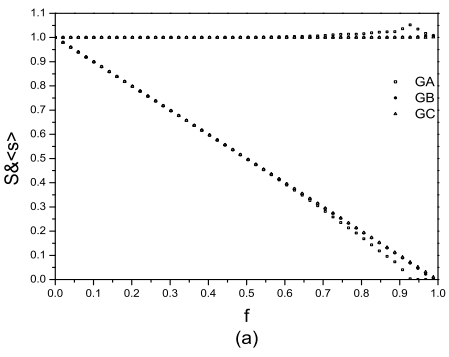

N=10
N=12
N=14
N=16
$(2\pi)^{1/2}\sigma P(l)$
$(l-<l>)/(2^{1/2}*\sigma)$

(b)

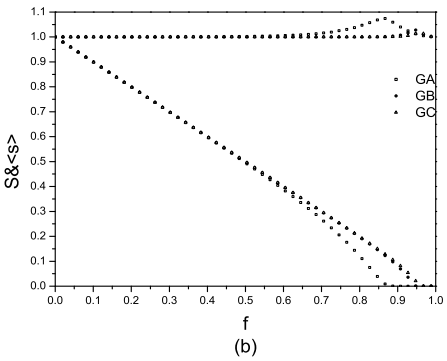

I
log(N)
(a)


I
log(N)
(c)


I
log(N)
(b)



(a)



(b)